Preclinical *In vivo* Study of New Insulin-Like Growth Factor-I Receptor–Specific Inhibitor in Ewing's Sarcoma

Maria C. Manara,[1] Lorena Landuzzi,[1] Patrizia Nanni,[2] Giordano Nicoletti,[1] Diana Zambelli,[1] Pier Luigi Lollini,[2] Cristina Nanni,[3] Francesco Hofmann,[4] Carlos García-Echeverría,[4] Piero Picci,[1] and Katia Scotlandi[1]

Abstract

Purpose: Small-molecule insulin-like growth factor-I receptor (IGF-IR)–specific tyrosine kinase inhibitors have been recently proposed as clinically viable approaches to impair IGF-IR functions. NVP-AEW541 seems one of the most promising agents. In this article, we point out its effects against migration, metastasis, vasculogenicity, and angiogenesis of Ewing's sarcoma cells.

Experimental Design: *In vivo* NVP-AEW541 effectiveness was analyzed against TC-71 Ewing's sarcoma growth and bone metastasis after cell inoculation in athymic mice. Activity of the compound against angiogenesis as well as vasculogenesis properties was also considered both *in vitro* and in xenografts. Serum glucose, urea, transaminase levels, as well as other signs of distress were checked in mice treated with the IGF-IR inhibitor.

Results: Significant inhibition of migration, metastasis, vasculogenicity, and angiogenesis was recorded after treatment of Ewing's sarcoma cells with NVP-AEW541. In view of its application and the similarity of insulin receptor and IGF-IR, diabetogenic side effects were considered. We observed a significant decrease of glucose blood serum due to increased glucose uptake at cellular level and an increase in urea concentration. Moreover, an initial weight loss was observed in mice bearing tumors. All these side effects were similarly detected in mice treated with vincristine. After the first days of treatment, all the animals started to grow again.

Conclusions: Our results globally reinforce the idea that IGF-IR inhibitor NVP-AEW541 could have a role in future combined therapies and suggest to pursue a thorough molecular analysis of the metabolic activity of IGF-IR to avoid possible side effects of these inhibitors.

There is compelling evidence that insulin-like growth factor (IGF)/IGF-I receptor (IGF-IR) system plays a major role in human neoplasias, and interfering with the IGF signaling system may be an attractive strategy for treatment of certain human cancers (1–3).

Biological functions of IGFs are initiated by their interactions with cell surface receptors, particularly the IGF-IR. IGF-IR is a tetramer consisting of two ligand-binding extracellular α-subunits and two β-subunits involving a transmembrane domain, an intracellular tyrosine kinase domain, and a COOH-terminal domain. The ligand-receptor interaction results in phosphorylation of tyrosine residues in the tyrosine kinase domain. Particularly, phosphorylation of Y1131, Y1135, and Y1136 induces conformational changes that allow substrate and ATP access to critical residues of the receptor. In turn, phosphorylation of adaptor proteins insulin receptor substrate 1-4 and Shc, the two major mediators of IGF-IR, leads to activation of phosphatidylinositol 3-kinase, mitogen-activated protein kinase, and 14-3-3 pathways (4–6).

IGF-IR is widely up-regulated in solid tumors and mediates many characteristics of malignant phenotype, including proliferation, protection from apoptosis, tumor cell motility, and hypoxic response. Moreover, IGF can protect cells from killing by a range of cytotoxic drugs, and IGF-IR activation is shown to mediate resistance to inhibitors of epidermal growth factor receptor and HER2 (7–12). Being able to influence many aspects of malignant phenotype, IGF-IR is emerging as a very promising therapeutic target. However, this targeted therapy will be successful only if the receptor is absolutely necessary for pathogenesis and tumor progression. In this context, Ewing's sarcoma may represent one of the best-characterized examples due to the large amount of data supporting the role of the receptor in invasion, angiogenesis, metastases, and drug resistance (13–16). IGF-IR is certainly required for maintenance of Ewing's sarcoma malignant phenotype, and therapies targeting the receptor may represent a valuable, urgently needed, adjuvant to conventional treatments.

Authors' Affiliations: [1]Laboratory of Oncologic Research, Istituti Ortopedici Rizzoli; [2]Cancer Research Section, Department of Experimental Pathology, University of Bologna; [3]UO Medicina Nucleare Azienda Ospedaliero-Universitaria di Bologna Policlinico S. Orsola-Malpighi, Bologna, Italy; and [4] Novartis Institutes for BioMedical Research, Novartis Pharma AG, Basel, Switzerland

Received 6/22/06; revised 10/25/06; accepted 11/30/06.

Grant support: Italian Association for Cancer Research (K. Scotlandi) and European Project EuroBoNet.

The costs of publication of this article were defrayed in part by the payment of page charges. This article must therefore be hereby marked *advertisement* in accordance with 18 U.S.C. Section 1734 solely to indicate this fact.

Requests for reprints: Katia Scotlandi, Laboratorio di Ricerca Oncologica, Istituti Ortopedici Rizzoli, Via di Barbiano 1/10, 40136 Bologna, Italy. Phone: 39-051-6366760; Fax: 39-051-6366761; E-mail: katia.scotlandi@ior.it.

doi:10.1158/1078-0432.CCR-06-1518

Recent development of small-molecule IGF-IR–specific tyrosine kinase inhibitors offers a promising opportunity for clinical use, thanks to their favorable pharmacokinetic properties, including solubility and stability and their oral bioavailability. Due to high levels of homology between IGF-IR and insulin receptor, particularly at tyrosine kinase domains (84% homology), development of truly selective inhibitors was delayed. However, there are now some very interesting and promising compounds, which may act as ATP (17, 18) or non-ATP antagonists (19, 20). We recently highlighted clinical potentialities of NVP-AEW541, a pyrrolopyrimidine derivative that exhibits a 27-fold selectivity to IGF-IR compared with insulin receptor, in sarcomas, particularly against Ewing's sarcoma (21). Here, we further extend the analysis of effectiveness of this compound, testing its activity against Ewing's sarcoma angiogenesis and metastasis ability. By assessing potential *in vivo* toxicity of NVP-AEW541, we also offer the necessary rationale for its use in possible forthcoming clinical trials.

Materials and Methods

Cells. Human Ewing's sarcoma cell lines (TC-71, 6647, SK-N-MC, and SKES-1), which express the insulin receptor and IGF-IR, and the human breast cancer cell line SK-BR-3, which expresses the insulin receptor but not IGF-IR, were cultured in Iscove's modified Dulbecco's medium (IMDM) plus 10% fetal bovine serum (FBS) supplemented with 20 units/mL penicillin, 100 μg/mL streptomycin (Sigma, St. Louis, MO), and 10% inactivated FBS (Cambrex Bioscience, Verviers, Belgium). Cells were maintained at 37°C in a humidified 5% CO_2 atmosphere. Primary cultures of human umbilical vascular endothelial cells (HUVEC) were isolated from recently collected unfrozen umbilical cords. Cells were grown in M199 medium (Sigma) supplemented with 20% FBS, 2 mmol/L L-glutamine (Sigma), 50 mg/mL endothelial cell growth supplement (Sigma), 100 mg/mL heparin (Sigma), and antibiotics as described previously (22). Cells were maintained at 37°C in 5% CO_2 atmosphere and used for experiments between the second and fourth passage.

Motility assay. Motility assay was done using Transwell chambers (Costar, Cambridge, MA) with 8-μm pore size, polyvinylpyrrolidone-free, polycarbonate filters (Nucleopore, Pleasanton, CA). IMDM plus 10% FBS alone or IMDM plus 10% FBS with IGF-I (50 ng/mL; Upstate, Lake Placid, NY) were placed in the lower compartment of the chamber. Ewing's sarcoma cells (10^5) were resuspended in IMDM plus 10% FBS with or without NVP-AEW541 (range, 0.3-3 μmol/L) and then seeded in the upper compartment. Chambers were incubated at 37°C in a humidified atmosphere containing 5% CO_2 for 18 h. Cells migrated toward the filter to reach the lower chamber base were counted after Giemsa staining. All experiments were done in triplicate.

Vascular endothelial growth factor-A assay. Production of vascular endothelial growth factor (VEGF)-A was also analyzed after 24 to 48 h of treatment of Ewing's sarcoma cells with NVP-AEW541 (0.3-1 μmol/L). Production of VEGF-A was measured using human VEGF immunoassay kit according to the manufacturer's instructions (Biosource, Camarillo, CA). Standard culture medium (IMDM 1% FBS) was analyzed as control.

Analysis of functional activity of VEGF-A on endothelial cells. HUVECs ($100{,}000/cm^2$) were seeded in uncoated plates in M199 complete medium. After 24 h, M199 medium was removed and HUVECs were incubated with VEGF-A–containing low-serum conditioned medium obtained from untreated Ewing's sarcoma cells (control) or Ewing's sarcoma cells treated for 24 and 48 h with NVP-AEW541 (0.3-1 μmol/L). To analyze cell growth, HUVEC growth was evaluated on harvested cells by trypan blue vital cell count every 24 h. Detection and quantification of apoptotic cells was also obtained by using flow cytometric analysis of Annexin V–labeled cells (Medical & Biological Laboratories, Naka-ku Nagaya, Japan). Simultaneous application of propidium iodide as DNA stain was used to discriminate necrotic from apoptotic cells.

Fluorescence analysis of glucose uptake. TC-71 and SK-BR-3 cells cultured on glass coverslips were serum depleted for 20 h and then exposed for 1 h to 0.3 μmol/L NVP-AEW541, 50 ng/mL insulin, or both. Fluorescent glucose analogue 6-[*N*-(7-nitrobenz-2-oxa-1,3-diazol-4-yl)amino]-6-deoxyglucose from Molecular Probes (Eugene, OR) was added in the medium at the final concentration of 30 μmol/L (23). DNA was stained with Hoechst 33342 (Sigma).

In vivo *treatments with NVP-AEW541.* Four- to 5-week-old female athymic Crl:C-1-*nu*/*nu* BR mice (Charles River Italia, Calco, Lecco, Italy) were used. Mice were treated according to the Institutional and European Union guidelines. Tumor growth was determined after s.c. injection of 5×10^6 TC-71 cells. Mice were randomized into controls and treated groups when tumors started to be measurable (6 days after cell inoculation, day 0 of treatment). Treatments were as follows: vehicle [25 mmol/L L(+)-tartaric acid; orally, twice daily, 7 days per week for 2 weeks], vincristine [alone i.p. (1 mg/kg/d) on days 0 and 1 of treatment], NVP-AEW541 [orally, alone, twice daily, 7 days per week for 2 weeks (50 or 100 mg/kg)], or NVP-AEW541 (50 mg/kg; orally, twice daily, 7 days per week) plus vincristine [i.p. (1 mg/kg/d) on days 0 and 1 of treatment]. Tumor growth was assessed weekly by measuring tumor volume, calculated as $\pi / 2 \cdot [\sqrt{v(ab)}]^3 / 6$, where a is the maximal tumor diameter and b is the tumor diameter perpendicular to a. For ethical reasons, mice with tumor were sacrificed when they reached a tumor volume of 2.5 cm^3 by CO_2 inhalation and necropsied. To evaluate NVP-AEW541 ability to inhibit metastatic ability of TC-71 cells, 2×10^6 viable cells were injected i.v. into a tail lateral vein. To obtain natural killer–depressed animals, mice were injected i.v. with 0.4 mL of 1:25 dilution of anti-asialo GM_1 antiserum (Wako, Düsseldorf, Germany) 24 h before cell inoculation. Ten to 15 mice per group were treated as follows: vehicle [25 mmol/L L(+)-tartaric acid; orally, twice daily, 7 days per week for 2 weeks], vincristine [alone i.p. (1 mg/kg/d) on days 0 and 1 of treatment], NVP-AEW541 [orally, alone, twice daily, 7 days per week for 2 weeks (50 mg/kg)], or NVP-AEW541 (50 mg/kg; orally, twice daily, 7 days per week) plus vincristine [i.p. (1 mg/kg/d) on days 0 and 1 of treatment]. Volume of bone metastases was assessed as described above for primary tumors. For ethical reasons, mice with local tumors/bone metastases were sacrificed when tumor volume was 2.5 cm^3. Mice that did not display evident bone metastases were sacrificed 3 months after cell inoculation and necropsied. The number of pulmonary metastases was determined by counting with a stereomicroscope after staining with black India ink. The [^{18}F]fluorodeoxyglucose positron emission tomography scan was also carried out for selected animals. Procedures were as follows: the animal was anesthetized with gas anesthesia (sevofluorane, 3-5%; oxygen, 1 L/min) and injected with 20 MBq of [^{18}F]fluorodeoxyglucose in a volume of 0.1 mL via the tail vein with an insulin syringe. The animal was subsequently allowed to wake up for the uptake time (60 min) and was free to move. Residual dose was measured to verify the effective dose injected. Finally, a second anesthesia was given in the same way to do the scan. Each anesthetized animal was put on the scanner bed in a prone position. Images were acquired with a Small Animal PET tomograph (eXplore Vista DR, GE Healthcare, Munich, Germany) for a total acquisition time of 20 min. As the axial field of view was 4 cm, one bed position was sufficient to cover the whole body. Once the scan was finished, gas anesthesia was interrupted and the animal was put in a recovery box with a warm temperature until complete recovery. Images were reconstructed with iterative reconstruction OSEM-2D and read in three cuts (axial, sagittal, and coronal).

Immunohistochemical analysis. Sections (5 μm) from formalin-fixed, paraffin-embedded tumor xenografts were placed on poly-L-lysine–coated slides (Sigma). Avidin-biotin-peroxidase procedure was used for immunostaining. Briefly, sections were treated sequentially with xylene and ethanol to remove paraffin. For immunohistochemical detection of IGF-IR and Ki-67, sections were pretreated with a citrate buffer solution

[0.01 mol/L citric acid and 0.01 mol/L sodium citrate (pH 6.0)] in a microwave oven at 750 W for three cycles of 5 min each. Endogenous peroxidase activity was blocked by treatment with 3% hydrogen peroxide in methanol for 30 min at room temperature. A blocking step with normal rabbit or goat serum (Vector, Burlingame, CA) was used. This treatment ensured antigen retrieval from samples. The following primary antibodies [anti-IGF-IR$_\beta$ (C-20; 1:50 dilution; Santa Cruz Biotechnology, Inc., Santa Cruz, CA), anti-CD31 (1:10 dilution), MIB-1 (1:100 dilution; Calbiochem-Novabiochem, San Diego, CA), anti-CD99 O13 monoclonal antibody (obtained commercially; 1:80 dilution; Signet, Dedham, MA), anti–phosphorylated Akt (Ser^{473}), and anti–phosphorylated p44/42 mitogen-activated protein kinase (Thr^{202}/Tyr^{204}; 1:100 dilution; Cell Signaling Technology, Inc., Beverly, MA)] were applied overnight in a moist chamber at 4°C. The following day, tissue sections were incubated with a secondary biotinylated anti-goat antibody and with an avidin-biotin-peroxidase complex (Vector). The final reaction product was revealed by exposure to 0.03% diaminobenzidine (Sigma), and nuclei were counterstained with Mayer's hematoxylin.

Serum glucose, urea, and transaminase levels. Six-week-old non–tumor-bearing nude mice were analyzed to verify whether NVP-AEW541 modulates serum levels of glucose and induces suffering at hepatic or systemic level. Three mice per group were treated with NVP-AEW541 (50/mg/kg, orally, twice daily) or with vincristine alone (1 mg/kg/d; on days 0 and 1). One week after beginning of treatment, mice were sampled for blood. Determination of serum concentration of glucose and other enzymes was done.

Statistical analysis. Differences among means were analyzed using Student's *t* test and ANOVA test. Kaplan-Meier and log-rank methods were used to draw and evaluate the significance of metastasis-free curves.

Results

NVP-AEW541 effects against tumor growth. NVP-AEW541 induced a dose-dependent reduction in local growth of TC-71 xenografts (Fig. 1A), especially with the dose of 100 mg/kg,

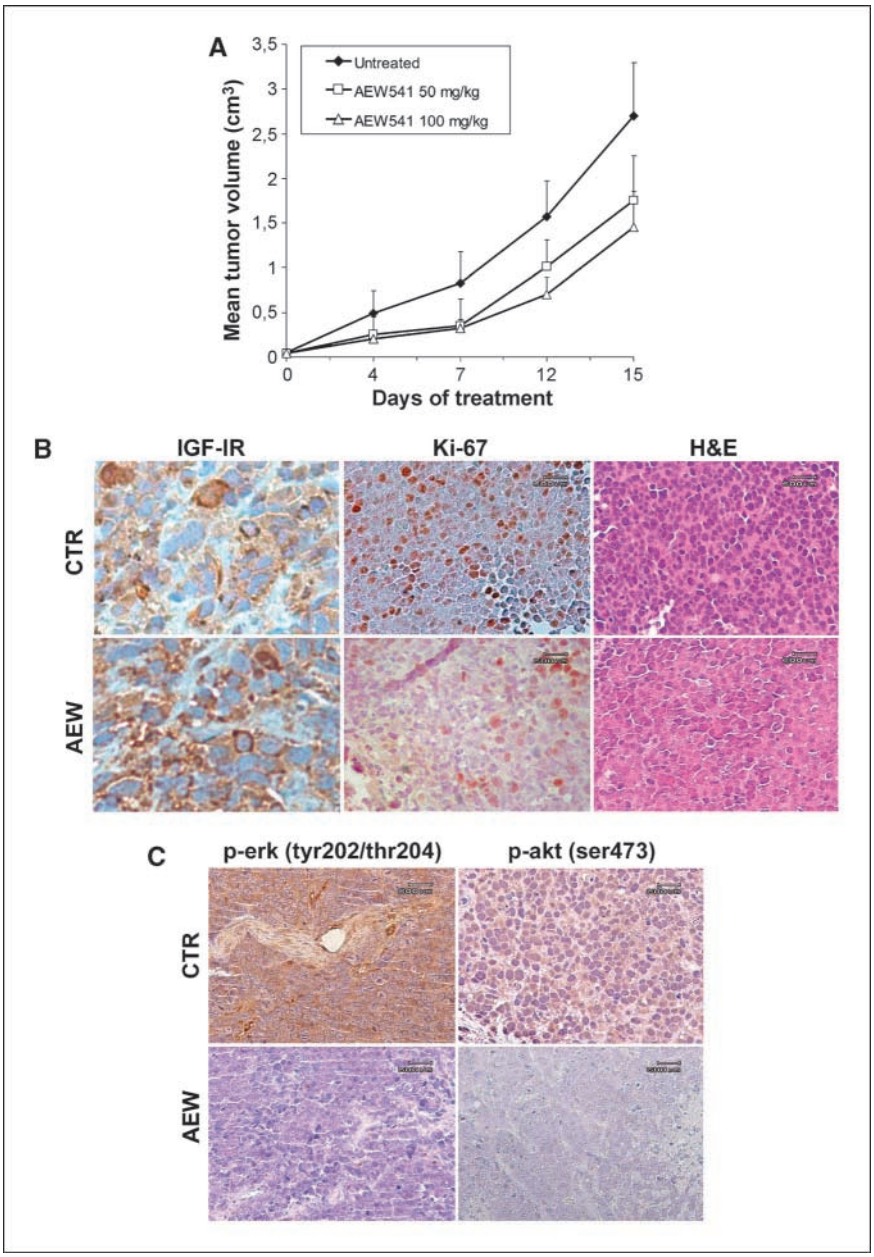

Fig. 1. *A,* inhibition of TC-71 tumor growth in nude mice by NVP-AEW541. *In vivo* growth curves of TC-71 tumors (5×10^6 s.c.) in groups of 10 athymic mice treated with vehicle [25 mmol/L L(+)-tartaric acid] or NVP-AEW541 (50 or 100 mg/kg) orally, twice daily, 7 d per week for 2 wks. Treatments began at day 6 after cell injection when tumors started to be measurable. *B,* immunohistochemical evaluation of IGF-IR or Ki-67 expression in untreated or NVP-AEW541–treated (100 mg/kg) mice. H&E staining was also used to evaluate cell morphology. *C,* immunohistochemical evaluation of phosphorylated extracellular signal-regulated kinase (*p-erk*) and phosphorylated Akt (*p-akt*) in untreated or NVP-AEW541–treated (100 mg/kg) mice.

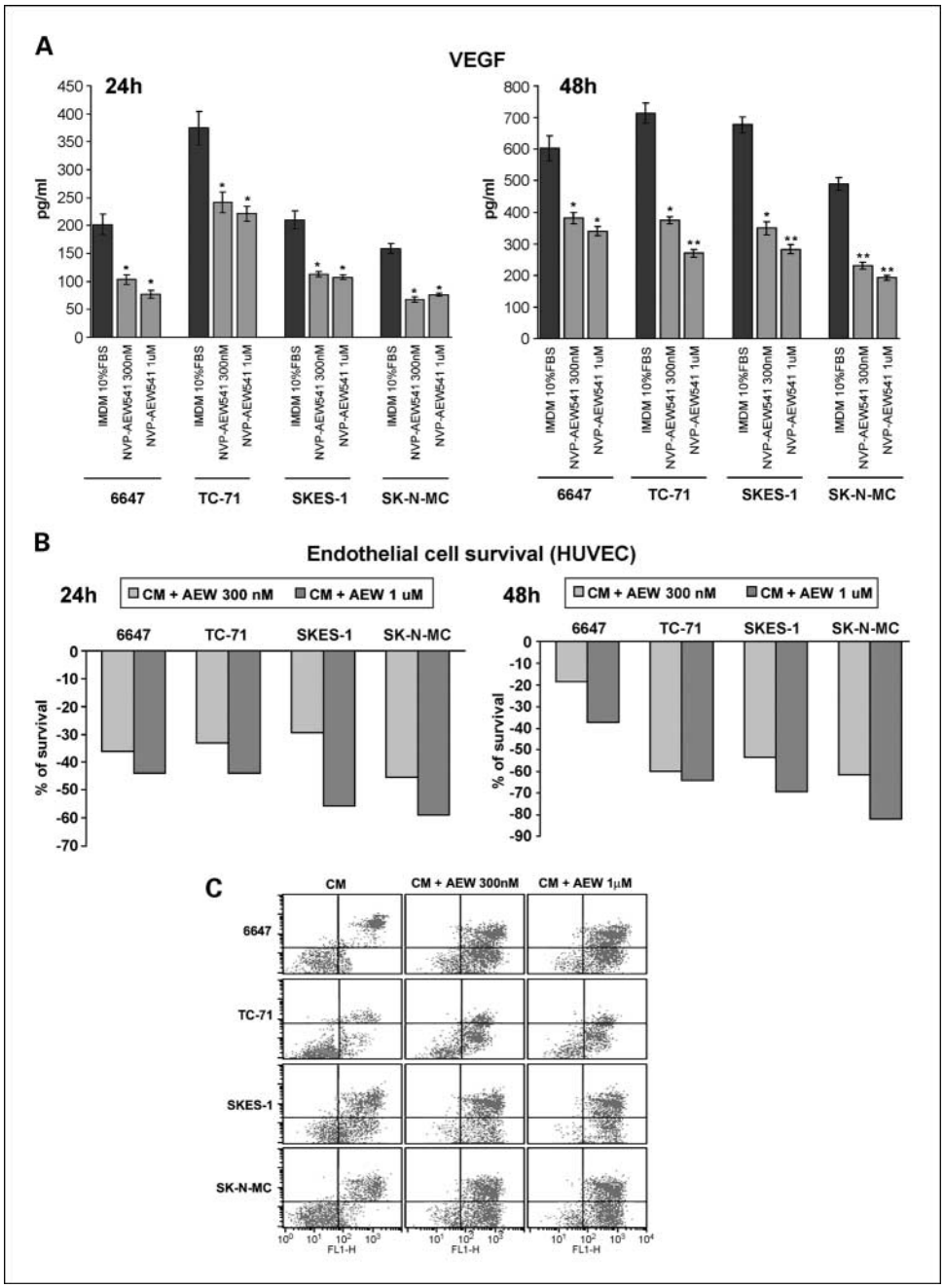

Fig. 2. Effects of NVP-AEW541 on VEGF expression and activity in Ewing's sarcoma cells. *A,* levels of VEGF-A, detected by ELISA, after 24 h (*left*) and 48 h (*right*) of exposure of Ewing's sarcoma cells to NVP-AEW541. Unconditioned medium was used as blank. Columns, mean of three experiments; bars, SE. *, $P < 0.05$, ANOVA test with respect to control; **, $P < 0.001$, ANOVA test with respect to control. *B,* VEGF-A activity measured by HUVEC proliferation assay. HUVECs were seeded in 24-well plates in standard medium and, the following day, incubated with VEGF-containing (see *A*) conditioned medium (*CM*) of Ewing's sarcoma – treated cells. After 24 h (*left*) and 48 h (*right*), HUVEC growth was evaluated by trypan blue vital cell count. Results shown as percentage of the control (HUVECs exposed to supernatants of Ewing's sarcoma – untreated cells). Representative results of two independent experiments. *C,* evaluation of apoptosis in HUVECs after 48 h of treatment with conditioned Ewing's sarcoma cell supernatants. Percentage of apoptotic cells was evaluated by flow cytometric analysis of Annexin V-FITC – labeled cells.

whereas lower doses of 50 mg/kg had statistical effect only in combination with vincristine (21). Contrary to what was reported with IGF-IR antibody (3), inhibition of kinase activity by NVP-AEW541 did not result in receptor down-regulation (Fig. 1B). Instead, NVP-AEW541 strongly inhibited the down-stream IGF-IR signaling pathways mitogen-activated protein kinase and phosphatidylinositol 3-kinase in xenografts (Fig. 1C). Although this type of activity maybe expected because NVP-AEW541 is an inhibitor of function rather than of expression, it may explain why the compound simply induces reduction of tumor growth rather than causing tumor regression. Indeed, it is generally accepted that, unless the receptor is down-regulated, apoptosis does not occur (3). Remarkable but not complete decrease of Ki-67 positivity in tumors treated with NVP-AEW541 (Fig. 1B) was in line with the cytostatic rather than cytotoxic effect of the inhibitor.

NVP-AEW541 effects against angiogenesis and vasculogenesis of Ewing's sarcoma cells. Several evidences have also indicated how disruption of IGF-IR functions may constitute an effective tool for control of neovascularization in tumors (24, 25). Therefore, we verified effectiveness of NVP-AEW541 against angiogenesis as well as vasculogenesis properties of Ewing's sarcoma cells. Exposure of different cell lines to NVP-AEW541 significantly reduced expression of VEGF-A at protein level both at 24 and 48 h (Fig. 2A). To confirm inhibitory effects of impairment of IGF-IR on VEGF-A production, a functional endothelial cell proliferation assay was also done. Medium from Ewing's sarcoma cells treated for 48 h with NVP-AEW541

(0.3 or 1 μmol/L), which contained decreased amount of VEGF-A (Fig. 2A), induced a significant reduction in survival of normal endothelial HUVECs after 24 and 48 h of exposure (Fig. 2B). Viability of HUVECs exposed to conditioned medium from untreated cells was used as control. Analysis of apoptosis by Annexin test confirmed that treatment of Ewing's sarcoma cells with NVP-AEW541 induced a remarkably higher percentage of apoptotic HUVECs (Fig. 2C). In addition to angiogenesis, Ewing's sarcomas are also characterized by the presence of blood lakes. These vascular structures have been recently described as a consequence of the vasculogenic mimicry ability of Ewing's sarcoma cells and described as independent from VEGF production (26). In xenografts, we found that cells lining the lakes showed typical aberrant nuclei of tumor cells (Fig. 3A) and did not label with endothelial marker CD31 but expressed CD99 (Fig. 3B), a marker of Ewing's sarcoma cells, indirectly confirming that they are the result of the vasculogenic mimicry ability of Ewing's sarcoma cells. NVP-AEW541 significantly inhibited the number of blood lakes in xenografts (Fig. 3C) and this may be of therapeutic value due to the prognostic relevance of this variable (27). Therefore, NVP-AEW541 inhibitor seems to substantially limit the trophic support of Ewing's sarcoma cells, affecting both angiogenesis and vasculogenic mimicry abilities.

NVP-AEW541 effects against migration and metastatization of TC-71 cells. Impairment of IGF-IR functions by NVP-AEW541 induced a significant inhibition of the migratory ability of Ewing's sarcoma cells both when complete medium alone was used as a chemoattractant or when IGF-I was added (Fig. 4A). Antimetastasis action of the compound was analyzed against bone metastases, which are a major clinical problem not only for Ewing's sarcoma patients but also for breast and prostate cancer patients, two tumors for which IGF-IR targeting therapies have been proposed (1, 2). I.v. inoculation of TC-71 cells results in the rapid appearance of large bone colonies and in a few lung metastases; therefore, it is a simple and useful model to investigate effectiveness of drugs on bone lesions. The route of injection is simple, the pattern of colonization is highly reproducible (28), and the presence of metastasis in bone is easy to evaluate. Of course, only experimental metastases could be evaluated and this may represent a limit. However, at best of our knowledge, no spontaneous bone metastases have been reported after s.c. or orthotopic injection of Ewing's sarcoma cells. A few animals were also checked with positron emission tomography for the presence of bone metastases, and no extra small lesions apart from those the operator could easily check by weekly controls or autopsy (data not shown) were seen. Oral administration of NVP-AEW541 (50 mg/kg, twice daily for 15 days) significantly delayed occurrence of detectable bone metastases in animals inoculated i.v. with TC-71 cells (Fig. 4B). In fact, the mean time of development of metastasis was 35 ± 2 days in the control group versus 45 ± 3 days in the group treated with IGF-IR inhibitor ($P = 0.02$, Student's t test; $n = 13$ for control and $n = 15$ for treated mice). Tumor growth rate of

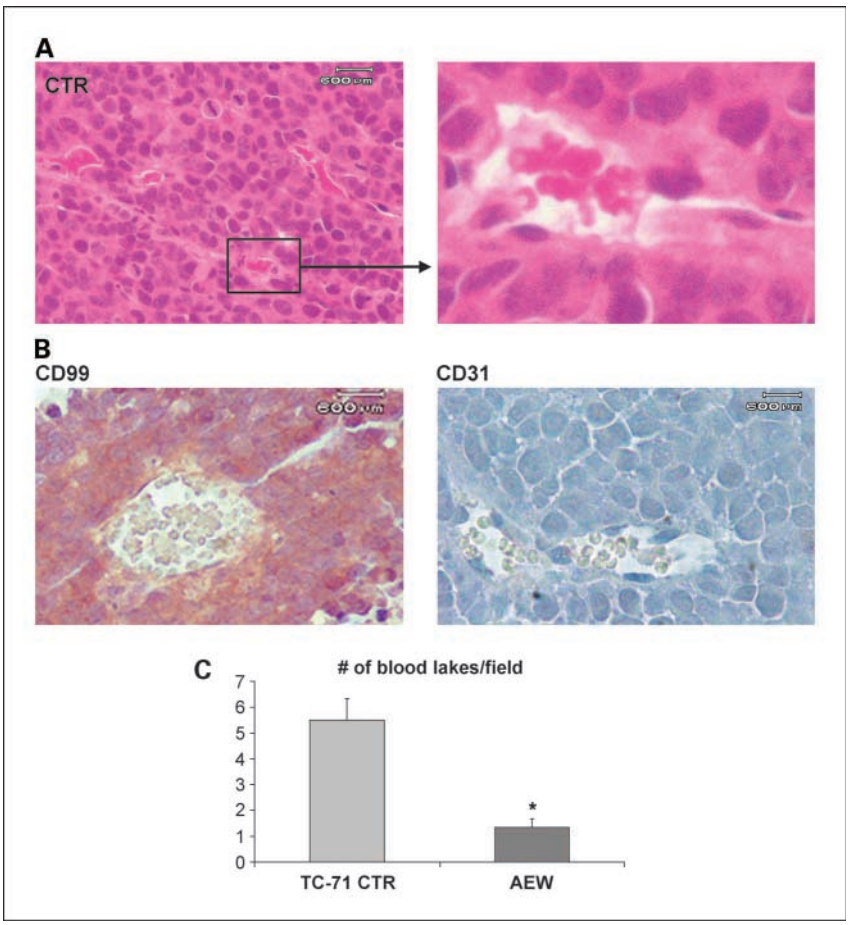

Fig. 3. Vasculogenic mimicry in Ewing's sarcoma and effects of NVP-AEW541. *A,* blood lakes highly present and easily recognizable in Ewing's sarcoma. *B,* vascular structures stained with CD99, a recognized marker of Ewing's sarcoma cells, but not with CD31, an endothelial marker. *C,* quantification of blood lakes in TC-71 – untreated or NVP-AEW541 – treated (50 mg/kg) tumors. *, $P < 0.05$, Student's t test with respect to control.

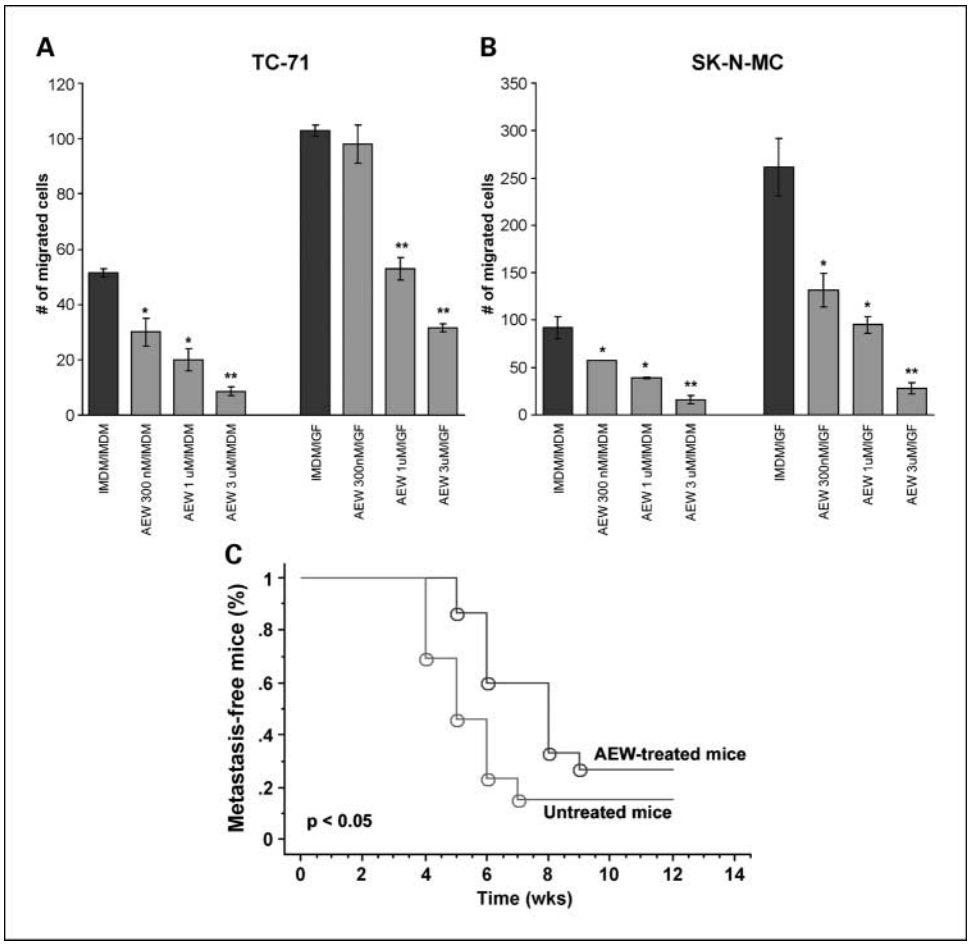

Fig. 4. *A,* effects of different doses of NVP-AEW541 on *in vitro* migration of Ewing's sarcoma cells. Cells (10^5) of TC-71 or SK-N-MC were incubated in the upper compartment of a Transwell chamber with or without the selective inhibitor. In the lower compartment, IMDM plus 10% FBS or IMDM plus 10% FBS and IGF-I (50 ng/mL) were used as source of chemoattractant. Column, mean of five independent experiments; bars, SE. *, $P < 0.05$, ANOVA test with respect to each corresponding control; **, $P < 0.001$, ANOVA test with respect to each corresponding control. *B,* delayed occurrence of bone metastases after treatment with NVP-AEW541 (50 mg/kg). Mice were treated twice daily, 7 d a week for 2 wks, after TC-71 cell inoculation starting from the day after tumor cell i.v. injection in the tail vein. *, $P < 0.05$, log-rank test.

bone lesions was also reduced, similarly to what was observed for primary tumors (data not shown).

Toxicologic profile of NVP-AEW541 in mice. Given the similarity between IGF-IR and insulin receptor kinase domains, normal tissue toxicity of small-molecule IGF-IR kinase inhibitors has to be considered. We monitored mice weight, glucose and urea concentrations in blood, and signs of hepatic distress during treatment. Significant weight loss was observed in mice bearing tumors, particularly during the first days of treatment (Fig. 5A). Weight loss was not related to the presence of tumors because we observed similar effects in non–tumor-bearing mice treated with the same doses of the compound (data not shown). After the first 6 days, mice started to regain weight and the trend of weight gain was similar to controls, indicating that animals overcame effects induced by initial administration of NVP-AEW541. No other detectable signs of suffering or deleterious effects were observed after impairment of IGF-IR by oral administration of 50 or 100 mg/kg of NVP-AEW541. Combination of NVP-AEW541 with vincristine increased reduction in mice weight, but again, after initial striking loss of weight, animals recovered and their weight curve substantially paralleled that of controls (Fig. 5B).

Nude mice were also analyzed to verify whether NVP-AEW541 modulates serum levels of glucose and induces liver toxicity. Due to weight alterations, we also checked blood urea concentration. Three mice per group were treated twice daily with NVP-AEW541 (50/mg/kg, orally) or with vincristine, and then, determination of serum concentration of glucose and other enzymes was done (Table 1). Mice treated with NVP-AEW541 did not show any diabetogenic effects, confirming that the compound does not inhibit insulin receptor activities but rather a statistically significant ($P < 0.05$) reduction in serum glucose concentration. An increase in urea concentration was also observed, likely due to increased catabolism in mice treated with the drug. No significant changes were detected for hepatic enzymes.

The lower serum glucose concentration may be due to an increased cellular uptake of glucose induced by NVP-AEW541. In fact, when fluorescent glucose analogue 6-[*N*-(7-nitrobenz-2-oxa-1,3-diazol-4-yl)amino]-6-deoxyglucose, a compound shown to be specific for glucose transporters (23), was used, fluorescence was clearly detected in cells treated with NVP-AEW541 or insulin (used as control), but there was no detectable glucose uptake in untreated cells (Fig. 5C). SK-BR-3 cells, lacking IGF-IR but expressing insulin receptor, were used as controls. They did not show increased uptake of glucose following NVP-AEW541, suggesting that NVP-AEW541–induced glucose uptake is dependent on IGF-IR.

Discussion

In a previous article, we showed that the small-molecule IGF-IR kinase inhibitor NVP-AEW541 has all the prerequisites for being considered a potential new drug for sarcomas (21).

In vitro effectiveness was proved and we identified the combination with vincristine, actinomycin D, and ifosfamide as the best drug-drug interactions. We here completed the preclinical analysis of its effectiveness by checking *in vivo* effects in terms of tumor growth, metastasis, angiogenesis, and vasculogenesis.

As expected, NVP-AEW541, orally given, twice daily for 2 weeks, did not induce down-regulation of IGF-IR. In general, successful mouse experiments have indicated that, for best results, it is necessary to induce down-regulation of the receptor. This is likely due to the fact that, unless the receptor is down-regulated, apoptosis does not occur (5). If this is correct, the mere inhibition of IGF-IR tyrosine kinase activity by small molecule would arrest tumor growth rather than causing tumor regression. Indeed, we observed a clear cytostatic but not cytotoxic effect on TC-71 tumor growth. However, this is not a crucial problem in terms of clinical attractiveness of this agent. Literature indicates that targeting IGF-IR sensitizes tumor cells to other anticancer agents, and we already showed that NVP-AEW541 acts synergistically in enhancing sensitivity of sarcoma cells to conventional chemotherapeutics both *in vitro* and *in vivo*. Therefore, the compound may still be very useful and indications are that it should be used as an adjuvant of chemotherapy.

A second indication that may be drawn from experimental evidence in literature and by our studies is that targeting of IGF-IR may be more effective on metastases (29–32). Here, we tested effectiveness of NVP-AEW541 against bone metastases. Patients with bone metastases invariably undergo an ominous clinical course. In fact, bone metastases represent a major cause of suffering and disability due to severe pain, pathologic fractures, disruption of neural function, or spinal cord compression. Moreover, treatment of patients with bone metastases is generally refractory to current therapeutic regimens. Taking advantage of a quite simple animal model, we showed that NVP-AEW541 significantly delayed occurrence of bone metastases and, similarly to effects observed in primary tumors, reduced growth of these lesions. This may be related either to antiproliferative actions against Ewing's sarcoma cells or to lower expression and production of VEGF-A in tumor cells after NVP-AEW541 treatment. VEGF, the most important angiogenesis factor, has been shown to stimulate bone resorption through its effects on osteoclasts (33, 34). Thus, Ewing's sarcoma cells reach the bone marrow space and then secrete VEGF, which facilitates osteolytic bone metastasis. VEGF may also facilitate tumor growth in bone by acting as an angiogenesis factor once invasion of bone is complete. Lower production of VEGF induced by NVP-AEW541 treatment may therefore reduce osteolysis induction, resulting in smaller bone lesions. We recognize that the metastasis model here used is somewhat artificial because all of the early steps of metastasis are bypassed. However, because IGF-IR inhibitor might also affect these early steps, the results might be even more impressive and realistic if a natural model could be analyzed. Unfortunately, suitable models of spontaneous lung and bone metastases are still lacking for sarcoma.

Together with antiangiogenesis effects through down-regulation of VEGF production, NVP-AEW541 was also shown to target vasculogenic structures, which derive from tumor cell plasticity of Ewing's sarcoma. It was recently shown how Ewing's sarcoma cells cooperate in the formation of a circulatory system that has been described as vasculogenic mimicry in aggressive melanoma. Vasculogenic mimicry, a process in which tumor cells gain characteristics normally restricted to endothelial cells (35), is abundantly present in Ewing's sarcoma as well as in other tumors and is also an indicator of poor prognosis in this neoplasm. Therefore, optimal treatment should require eradication of vasculogenic

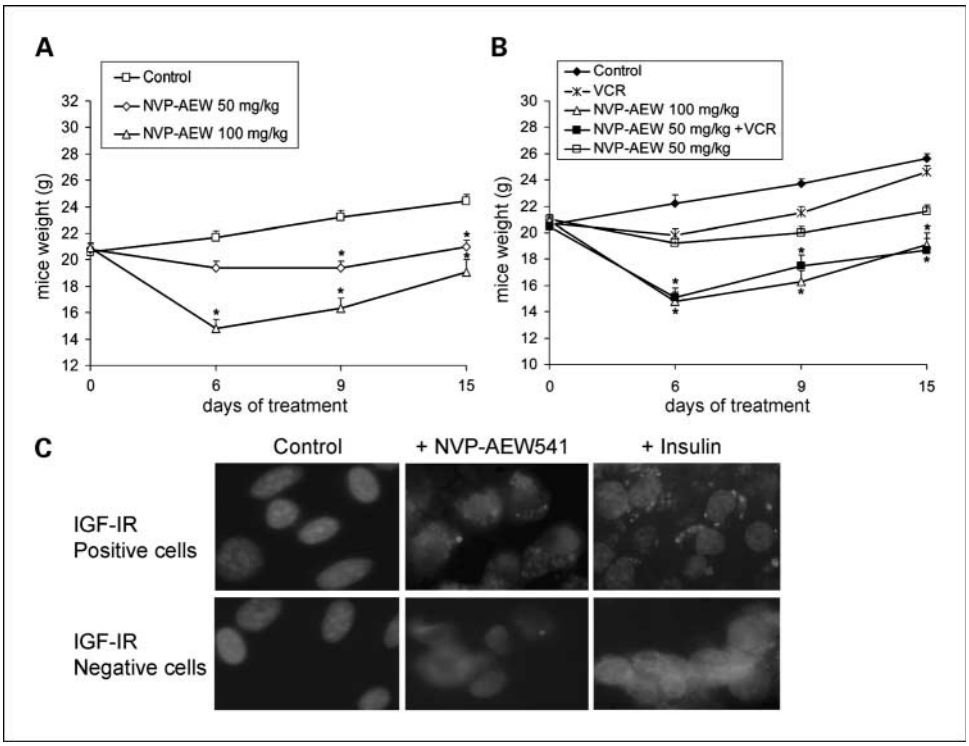

Fig. 5. *A* and *B*, weight variations in athymic mice treated with the following: vehicle [25 mmol/L L(+)-tartaric acid; orally, twice daily, 7 d per week for 2 wks], vincristine [*VCR*; alone i.p. (1 mg/kg/d) on days 0 and 1 of treatment], NVP-AEW541 [orally, alone, twice daily, 7 d per week for 2 wks (50 or 100 mg/kg)], or NVP-AEW541 (50 mg/kg; orally, twice daily, 7 d per week) plus vincristine [i.p. (1 mg/kg/d) on days 0 and 1 of treatment]. Treatments began when tumors started to be measurable. *, $P < 0.05$, ANOVA test. *C*, glucose uptake in cells treated with insulin or NVP-AEW541. Ewing's sarcoma cells, which express either IGF-IR or insulin receptor, or SK-BR-3 cells, which express the insulin receptor but not IGF-IR, were starved for 24 h and then treated for 1 h with insulin (50 ng/mL) or NVP-AEW541 (0.3 μmol/L). Fluorescence was detected immediately after adding fluorescence-labeled glucose analogue 6-[*N*-(7-nitrobenz-2-oxa-1,3-diazol-4-yl)amino]-6-deoxyglucose.

Table 1. Blood samples of mice treated with either NVP-AEW541 or vincristine

Samples	Urea (mg/dL)	Glucose (mg/dL)	Triglycerides (mg/dL)	AST (IU/L)	ALT (IU/L)
Control	49 ± 4	77 ± 12	97 ± 21	94 ± 33	29 ± 7
NVP-AEW541	76 ± 9*	34 ± 8*	97 ± 22	106 ± 15	22 ± 16
Vincristine	74 ±16	20 ± 18	149 ± 24	169 ± 23	24 ± 10

NOTE: Mice were sampled for blood 1 wk after the beginning of treatments (mean ± SE).
Abbreviations: AST, aspartate aminotransferase; ALT, alanine aminotransferase.
*$P \leq 0.05$, Student's t test.

tube formation either by inhibiting angiogenesis or by directly targeting tumor cells that participate in the formation of blood lakes. Treatment with NVP-AEW541 was effective in reducing the number of vascular lakes. Therefore, the drug affects tumor growth exhibiting activity against different crucial processes of malignancy.

The last aspect tackled in this article is the evaluation of possible toxic effects of NVP-AEW541. In general, all anti-IGF-IR strategies tested in animals have given little toxicity, supporting the usefulness of these agents. The problem with IGF-IR tyrosine kinase inhibitors is the very high homology between tyrosine kinase domains of IGF-IR and insulin receptor (5). NVP-AEW541 has, however, a 27-fold selectivity for IGF-IR versus the insulin receptor in cellular autophosphorylation assays (18), and our findings substantially confirm the high level of specificity of the IGF-IR inhibitor. Theoretical risk of IGF-IR inhibitors is to induce coinhibition of insulin receptor functions, which may result in diabetogenesis, an unacceptable effect. No increase in glucose serum concentration was observed but rather a significant decrease that may be due to increased glucose uptake induced at cellular level by NVP-AEW541. NVP-AEW541 – induced glucose uptake seemed to be limited to cells expressing IGF-IR and was not observed when only insulin receptor was present.

The conventional idea is that IGF-IR is mainly devoted to mediate growth, proliferation, and protection against apoptosis, whereas insulin receptor is responsible for metabolic functions. However, several lines of evidence also sustain direct involvement of IGF-IR in glucose uptake (36). In addition, studies on genetically modified mice have clearly shown how IGF axis is responsible for 50% to 60% of normal growth, although all these functions are still poorly characterized at molecular levels (37). Here, we observed a clear alteration of metabolic functions of the receptor following inhibition of its tyrosine kinase domain and showed that IGF-IR inhibition at certain conditions may have antidiabetic effects. The decreased glucose serum concentration is associated with increased serum levels of urea and with a remarkable decrease in mice weight that was particularly evident in the first days of treatment. Weight reduction was not previously observed when NVP-AEW541 was tested *in vivo*. It is possible that discrepancies are related with use in this case of very young animals (4-5 weeks). Younger animals were used because these are comparable in terms of general growth to puberty in mankind. Therefore, weight reduction in the animals may reflect impairment of growth hormone and IGF system in a period of life that is particularly sensitive to the action of these hormones and growth factors. These possible side effects should be kept in mind, particularly if the drug is to be used in young patients, and further molecular studies are necessary to better identify metabolic activities of the receptor. Considering that inhibition of tyrosine kinase domain does not result in loss of all IGF-IR activities, one could speculate that NVP-AEW541 can switch IGF-IR functions from mitogenesis to metabolism.

Taken together, we further showed the potential for effectiveness of IGF-IR signaling inhibitor NVP-AEW541 in cancer treatment, pointing out its effects against migration, metastatization, vasculogenesis, and angiogenesis. We also highlighted metabolic alterations in mice following treatment with the compound. Despite that this issue may be a concern, it is important also to acknowledge that animals overcame initial weight loss showing a trend of growth increase similar to controls and no other major signs of suffering were seen. In addition, alterations of glucose and urea serum concentrations were similar to those observed in mice treated with vincristine, a commonly used compound. So these side effects may be included in those that clinicians already deal with. Nevertheless, a better molecular understanding of metabolic activities of IGF-IR is necessary before planning the use of these compounds in clinical trials. It must be kept in mind that several other clinically viable alternative approaches exist. There are non – ATP-competitive IGF-IR kinase inhibitors under development (19) as well as a variety of anti-IGF-IR antibodies (38). Detailed analysis of the side effects of these agents is mandatory considering the high probability that IGF-IR modulators may lead to clinical trials.

Acknowledgments

We thank Alba Balladelli for revision of the manuscript and Dr. Loredana Pratelli for the enzymatic tests.

References

1. Jerome L, Shiry L, Leyland-Jones B. Deregulation of the IGF axis in cancer: epidemiological evidence and potential therapeutic interventions. Endocr Relat Cancer 2003;10:561 – 78.
2. Larsson O, Girnita A, Girnita L. Role of insulin-like growth factor 1 receptor signalling in cancer. Br J Cancer 2005;92:2097 – 101.
3. Baserga R. The insulin-like growth factor-I receptor as a target for cancer therapy. Expert Opin Ther Targets 2005;9:753 – 68.
4. LeRoit CT, Roberts CT, Jr. The insulin-like growth factor system and cancer. Cancer Lett 2003;195:127 – 37.
5. Baserga R, Peruzzi F, Reiss K. The IGF-1 receptor in cancer biology. Int J Cancer 2003;107:873 – 7.

6. Yu H, Rohan T. Role of the insulin-like growth factor family in cancer development and progression. J Natl Cancer Inst 2000;92:1472–89.

7. Dunn SE, Hardman RA, Kari FW, Barrett JC. Insulin-like growth factor 1 (IGF-1) alters drug sensitivity of HBL100 human breast cancer cells by inhibition of apoptosis induced by diverse anticancer drugs. Cancer Res 1997;57:2687–93.

8. Geier A, Beery R, Haimsohn M, Karasik A. Insulin-like growth factor-1 inhibits cell death induced by anticancer drugs in the MCF-7 cells: involvement of growth factors in drug resistance. Cancer Invest 1995;13:480–6.

9. Benini S, Manara MC, Baldini N, et al. Inhibition of insulin-like growth factor I receptor increases the antitumor activity of doxorubicin and vincristine against Ewing's sarcoma cells. Clin Cancer Res 2001;7:1790–7.

10. Lu Y, Zi X, Zhao Y, Mascarenhas D, Pollak M. Insulin-like growth factor-I receptor signaling and resistance to trastuzumab (Herceptin). J Natl Cancer Inst 2001;93:1852–7.

11. Chakravarti A, Chakladar A, Delaney MA, Latham DE, Loeffler JS. The epidermal growth factor receptor pathway mediates resistance to sequential administration of radiation and chemotherapy in primary human glioblastoma cells in a RAS-dependent manner. Cancer Res 2002;62:4307–15.

12. Scotlandi K, Manara MC, Hattinger CM, et al. Prognostic and therapeutic relevance of HER2 expression in osteosarcoma and Ewing's sarcoma. Eur J Cancer 2005;41:1349–61.

13. Scotlandi K, Benini S, Nanni P, et al. Blockage of insulin-like growth factor-I receptor inhibits the growth of ES in athymic mice. Cancer Res 1998;58:4127–31.

14. Scotlandi K, Maini C, Manara MC, et al. Effectiveness of insulin-like growth factor I receptor antisense strategy against Ewing's sarcoma cells. Cancer Gene Ther 2002;9:296–307.

15. de Alava E, Panizo A, Antonescu CR, et al. Association of EWS-FLI1 type 1 fusion with lower proliferative rate in Ewing's sarcoma. Am J Pathol 2000;156:849–55.

16. Toretsky JA, Kalebic T, Blakesley V, LeRoith D, Helman LJ. The insulin-like growth factor-I receptor is required for EWS/FLI-1 transformation of fibroblasts. J Biol Chem 1997;272:30822–7.

17. Mitsiades CS, Mitsiades NS, McMullan CJ, et al. Inhibition of the insulin-like growth factor receptor-1 tyrosine kinase activity as a therapeutic strategy for multiple myeloma, other hematologic malignancies, and solid tumors. Cancer Cell 2004;5:221–30.

18. Garcia-Echeverria C, Pearson MA, Marti A, et al. *In vivo* antitumor activity of NVP-AEW541—a novel, potent, and selective inhibitor of the IGF-IR kinase. Cancer Cell 2004;5:231–9.

19. Girnita A, Girnita L, del Prete F, Bartolazzi A, Larsson O, Axelson M. Cyclolignans as inhibitors of the insulin-like growth factor-1 receptor and malignant cell growth. Cancer Res 2004;64:236–42.

20. Menu E, Jernberg-Wiklund H, Stromberg T, et al. Inhibiting the IGF-1 receptor tyrosine kinase with the cyclolignan PPP: an *in vitro* and *in vivo* study in the 5T33MM mouse model. Blood 2006;107:655–60.

21. Scotlandi K, Manara MC, Nicoletti G, et al. Antitumor activity of the insulin-like growth factor-I receptor kinase inhibitor NVP-AEW541 in musculoskeletal tumors. Cancer Res 2005;65:3868–76.

22. Spisni G, Bartolini M, Orlandi B, Belletti S, Santi V, Tomasi V. Prostacyclin (PG12) synthase is a constitutively expressed enzyme in human endothelial cells. Exp Cell Res 1995;219:507–13.

23. Aller CB, Ehmann S, Gilman-Sachs A, Snyder AK. Flow cytometric analysis of glucose transport by rat brain cells. Cytometry 1997;27:262–8.

24. Strammiello R, Benini S, Manara MC, et al. Impact of IGF-I/IGF-IR circuit on the angiogenetic properties of Ewing's sarcoma cells. Horm Metab Res 2003;12:675–84.

25. Stoeltzing O, Liu W, Reinmuth N, et al. Regulation of hypoxia-inducible factor-1α vascular endothelial growth factor, and angiogenesis by an insulin-like growth factor-I receptor autocrine loop in human pancreatic cancer. Am J Pathol 2003;163:1001–11.

26. Holzer G, Obermair A, Koschat M, Preyer O, Kotz R, Trieb K. Concentration of vascular endothelial growth factor (VEGF) in the serum of patients with malignant bone tumors. Med Pediatr Oncol 2001;36:601–4.

27. van der Schaft DW, Hillen F, Pauwels P, et al. Tumor cell plasticity in Ewing sarcoma, an alternative circulatory system stimulated by hypoxia. Cancer Res 2005;65:11520–8.

28. Scotlandi K, Benini S, Manara MC, et al. Murine model for skeletal metastases of Ewing's sarcoma. J Orthop Res 2000;18:959–6.

29. Dunn SE, Ehrlich M, Sharp NJ, et al. A dominant negative mutant of the insulin-like growth factor-I receptor inhibits the adhesion, invasion, and metastasis of breast cancer. Cancer Res 1998;58:3353–61.

30. Long L, Rubin R, Baserga R, Brodt P. Loss of the metastatic phenotype in murine carcinoma cells expressing an antisense RNA to the insulin-like growth factor receptor. Cancer Res 1995;55:1006–9.

31. Scotlandi K, Avnet S, Benini S, et al. Expression of an IGF-I receptor dominant negative mutant induces apoptosis, inhibits tumorigenesis, and enhances chemosensitivity in Ewing's sarcoma cells. Int J Cancer 2002;101:11–6.

32. Sachdev D, Hartell JS, Lee AV, Zhang X, Yee D. A dominant negative type I insulin-like growth factor receptor inhibits metastasis of human cancer cells. J Biol Chem 2004;279:5017–24.

33. Nakagawa M, Kaneda T, Arakawa T, et al. Vascular endothelial growth factor (VEGF) directly enhances osteoclastic bone resorption and survival of mature osteoclasts. FEBS Lett 2000;473:161–4.

34. Aldridge SE, Lennard TW, Williams JR, Birch MA. Vascular endothelial growth factor receptors in osteoclast differentiation and function. Biochem Biophys Res Commun 2005;335:793–8.

35. Folberg R, Maniotis AJ. Vasculogenic mimicry. APMIS 2004;112:508–25.

36. Shefi-Friedman L, Wertheimer E, Shen S, Bak A, Accili D, Sampson SR. Increased IGFR activity and glucose transport in cultured skeletal muscle from insulin receptor null mice. Am J Physiol Endocrinol Metab 2001;281:E16–24.

37. Lamothe B, Baudry A, Desbois P, et al. Genetic engineering in mice: impact on insulin signalling and action. Biochem J 1998;335:193–204.

38. Surmacz E. Growth factor receptors as therapeutic targets: strategies to inhibit the insulin-like growth factor I receptor. Oncogene 2003;22:6589–97.

Clinical Cancer Research

Preclinical *In vivo* Study of New Insulin-Like Growth Factor-I Receptor–Specific Inhibitor in Ewing's Sarcoma

Maria C. Manara, Lorena Landuzzi, Patrizia Nanni, et al.

Clin Cancer Res 2007;13:1322-1330.